

IRRATIONAL ROTATIONS AND 2-FILLING RAYS

LVZHOU CHEN AND ALEXANDER J. RASMUSSEN

ABSTRACT. We study a skew product transformation associated to an irrational rotation of the circle $[0, 1]/\sim$. This skew product keeps track of the number of times an orbit of the rotation lands in the two complementary intervals of $\{0, 1/2\}$ in the circle. We show that under certain conditions on the continued fraction expansion of the irrational number defining the rotation, the skew product transformation has certain dense orbits. This is in spite of the presence of numerous non-dense orbits. We use this to construct laminations on infinite type surfaces with exotic properties. In particular, we show that for every infinite type surface with an isolated planar end, there is an *infinite* clique of 2-filling rays based at that end. These 2-filling rays are relevant to Bavard–Walker’s *loop graphs*.

1. INTRODUCTION

Our goal in this paper is to study skew products over irrational rotations on the circle and to explore relationships to laminations on infinite type surfaces. In particular, we prove that specific orbits are dense in a collection of skew product transformations. We use this to show that certain laminations on infinite type surfaces have dense boundary leaves. Finally, we use this to construct certain rays on infinite type surfaces with exotic properties, which are relevant to the study of Bavard–Walker’s *loop graphs*.

We consider the circle S^1 as the closed unit interval $[0, 1]$ with 0 and 1 identified. For a number $\alpha \in [0, 1)$, we define the rotation $t = t_\alpha : S^1 \rightarrow S^1$ by $t(x) = x + \alpha$ modulo 1. We define the function $f : S^1 \rightarrow \mathbb{R}$ by $f = \chi_{[0, 1/2)} - \chi_{[1/2, 1)}$ where χ_E denotes the characteristic function of the set E in question. We define a resulting skew product transformation $T = T_\alpha : S^1 \times \mathbb{Z} \rightarrow S^1 \times \mathbb{Z}$ by

$$T(x, s) := (tx, s + fx) = (x + \alpha, s + fx).$$

We endow \mathbb{Z} with the discrete topology and $S^1 \times \mathbb{Z}$ with the resulting product topology. We consider the continued fraction expansion for α ,

$$\alpha = [0; a_1, a_2, \dots] = \frac{1}{a_1 + \frac{1}{a_2 + \frac{1}{a_3 + \dots}}}.$$

We prove:

Theorem 1.1. *Suppose that the continued fraction expansion $\alpha = [0; a_1, a_2, \dots]$ satisfies that $a_1 \geq 5$ is odd and $a_n \geq 6$ is even for every $n > 1$. Then, for any $s \in \mathbb{Z}$, the (forward) orbit $\{T^n(1/2, s)\}_{n=0}^\infty$ is dense in $S^1 \times \mathbb{Z}$.*

Note that for any $n \geq 0$, $T^n(x, s) = (t^n x, s + S_n(x))$ where $S_n(x) = \sum_{i=0}^{n-1} f(t^i x)$ is the n^{th} Birkhoff sum for x . For any $m \in \mathbb{Z}$, we consider the set $\Sigma(x, m) := \{n \in \mathbb{Z}_{\geq 0} : S_n(x) = m\}$ of times n at which $S_n(x)$ is equal to m . Denote by $k + \Sigma(x, m)$ the set above translated by $k \in \mathbb{Z}$. The following corollary, when $k = 0$, is a restatement of Theorem 1.1. The general case, which is useful for our applications, also quickly follows from Theorem 1.1; see the next section for its proof.

Corollary 1.2. *Suppose that the continued fraction expansion $\alpha = [0; a_1, a_2, \dots]$ satisfies that $a_1 \geq 5$ is odd and $a_n \geq 6$ is even for every $n > 1$. Then, for any $k, m \in \mathbb{Z}$, the partial orbit $\{t^n(1/2)\}_{n \in k + \Sigma(1/2, m)}$ is dense in S^1 .*

In particular, for any $m \in \mathbb{Z}$, there are infinitely many $n \geq 0$ with $S_n(1/2) = m$. In contrast, it is shown in [6, Theorem 1] (by the characterization of \mathcal{H}_2) that $S_n(1/2) < 0$ for all $n \geq 1$ if $\alpha = [0; a_1, a_2, \dots]$ with a_i even for all i odd. In addition, for almost every α , there is an uncountable set (with Hausdorff dimension equal to some constant $c \in (0, 1)$ independent of α) of initial points $x \in [0, 1)$ with $S_n(x) \leq 0$ for all $n \geq 1$ [8].

We use our results above to construct examples of interesting laminations and rays on infinite type surfaces. For the first statement, recall that a complete hyperbolic surface X is of the *first kind* if it is equal to its convex core. A geodesic lamination Λ on X is *topologically transitive* if it contains a leaf which is dense in Λ .

Theorem 1.3. *Let S be any orientable infinite type surface with at least one isolated puncture. Then there is a hyperbolic surface X of the first kind homeomorphic to S , and a geodesic lamination Λ on X , such that Λ is topologically transitive, with infinitely many leaves which are not dense in Λ .*

For our second application, we consider the *loop graph* $L(S; p)$ of an infinite type surface S with an isolated puncture p , defined by Bavard in [2] and studied further by Bavard–Walker in [4] and [5]. The vertices of $L(S; p)$ are the simple, essential loops on S asymptotic to p on both ends, considered up to isotopy. Two isotopy classes are joined by an edge when the corresponding isotopy classes can be realized disjointly. The graph $L(S; p)$ is Gromov-hyperbolic and of infinite diameter [5]; see also [1]. Bavard–Walker [5] identified the points on the Gromov boundary of $L(S; p)$ with cliques of the so-called high-filling rays. As a related notion, a *2-filling ray* ℓ on S is a kind of *fake boundary point* for $L(S; p)$. Namely, such a ray is asymptotic to p , and intersects every loop on S , so that it has strong filling properties similar to high-filling rays, but it is not high-filling. See Section 3 for the precise definitions.

Bavard–Walker asked in [4, Question 2.7.7] whether 2-filling rays exist, for instance, when S is the plane minus a Cantor set. This was answered affirmatively by the authors in [7]. Such 2-filling rays always come organized into families of mutually disjoint 2-filling rays called *cliques*. The authors showed that the cliques can have any finite cardinality in [7, Theorem 5.1], and asked whether such cliques can be infinite [7, Question 5.7]. We answer this question affirmatively in Theorem 1.4 below for any infinite type surface S with an isolated puncture. In particular, 2-filling rays exist on all such surfaces. The analogous problem about the size of cliques of high-filling rays has been solved by methods different from our dynamical approach: such a clique can be of any finite cardinality on any infinite type surface S with an isolated puncture by [4, Theorem 8.1.3], and it can also be infinite at least when S is the plane minus a Cantor set by [3].

Theorem 1.4. *Let S be an orientable infinite type surface with at least one isolated puncture p . Then there exists an infinite clique of 2-filling rays on S based at p .*

It is an open problem to describe the boundaries of the loop graphs $L(S; p)$ as spaces of geodesic laminations. The authors believe that solving this problem would lead to significantly better understanding of the graphs $L(S; p)$. The existence of exotic laminations and rays as constructed in Theorem 1.3 and Theorem 1.4 and in [7] point to the difficulty of solving this problem and to the complexity of the graphs $L(S; p)$. It would be interesting to use skew products to construct other interesting laminations and mapping classes of infinite type surfaces.

Acknowledgments. We owe a debt of gratitude to Jon Chaika for teaching us and suggesting the method used in this paper for studying irrational rotations. We also thank the anonymous referee for their careful reading of the paper and suggestions. The second author was partially funded by NSF grant DMS-2202986.

2. PROOF OF THEOREM 1.1

We choose $\alpha = [0; a_1, a_2, \dots]$ satisfying the conditions of Theorem 1.1; i.e. $a_1 \geq 5$ is odd and $a_i \geq 6$ is even for every $i \geq 2$. Furthermore we set $\alpha_1 = \alpha$ and for $i \geq 2$,

$$(2.1) \quad \alpha_i = [0; a_i - 1, a_{i+1}, a_{i+2}, \dots].$$

Let

$$G(x) = \frac{1}{x} - \left\lfloor \frac{1}{x} \right\rfloor$$

be the Gauss transformation. Then $\alpha_{i+1} = G(\alpha_i)/(1 - G(\alpha_i))$.

Our method of proof considers first return maps to certain subintervals, which shares some similarity with the renormalization procedure used in related work; see [8] for instance, which also gives insights about the behavior of other orbits.

We will compute a sequence of nested intervals $[0, 1) = I_1 \supset I_2 \supset I_3 \supset \dots$ each centered at $1/2$ and the first return maps to I_i . Let

$$k_i : I_i \rightarrow \mathbb{N}, \quad k_i(x) = \inf\{k > 0 : t^k x \in I_i\}$$

be the first return time to I_i and

$$\bar{t}_i : I_i \rightarrow I_i, \quad \bar{t}_i(x) = t^{k_i(x)}(x)$$

be the first return map. Our construction guarantees the following properties, which we will verify later.

- (1) \bar{t}_i is rotation by $(-1)^{i+1}\alpha_i$ (rescaled by the length of I_i).
- (2) Moreover, we compute the induced Birkhoff sums

$$\bar{f}_i : I_i \rightarrow \mathbb{Z}, \quad \bar{f}_i(x) = \sum_{j=0}^{k_i(x)-1} f(t^j x);$$

i.e. \bar{f}_i records the Birkhoff sum accumulated before a point in I_i returns to I_i under iteration of t . Then by our construction \bar{f}_i will be equal to $+1$ on the sub-interval of points to the left of $1/2$ and -1 on the sub-interval of points to the right of $1/2$.

Theorem 1.1 is a consequence of the following, seemingly weaker proposition.

Proposition 2.1. *There is a sequence of intervals $[0, 1) = I_1 \supset I_2 \supset I_3 \supset \dots$ such that:*

- (1) I_i contains $1/2$ for each i and is symmetric about $1/2$ for each i ;
- (2) for each $i \geq 1$ the interval I_{i+1} has length $|I_{i+1}| \leq \alpha_i |I_i|$;
- (3) for each $i \geq 2$, after rescaling I_i by $1/|I_i|$, the function $\bar{f}_i(x)$ is equal to $\chi_{[0, 1/2)} - \chi_{[1/2, 1)}$;
- (4) for any i , and for any $m \in \mathbb{Z}$, there exists an orbit point $t^k(1/2) \in I_i$, for some $k \in \mathbb{Z}_+$, with $S_k(1/2) = m$.

Proof of Theorem 1.1 assuming Proposition 2.1. First we improve the last bullet point to the following claim: for any $m \in \mathbb{Z}$ there exist orbit points $t^k(1/2)$ in I_i to the right of $1/2$ with $S_k(1/2) = m$ and similarly there exist points $t^k(1/2)$ to the left of $1/2$ with $S_k(1/2) = m$, $k \in \mathbb{Z}_+$. We focus on the case of finding points to the right of $1/2$, as the other case is analogous.

Choose i odd, so that the first return to I_i is rotation by $\alpha_i = [0; a_i - 1, a_{i+1}, a_{i+2}, \dots]$. For any $m \in \mathbb{Z}$, there is some $k \in \mathbb{Z}_+$ such that $t^k(1/2) \in I_{i+1}$ with $S_k(1/2) = m$. If $t^k(1/2)$ lies to the right of $1/2$ then there is nothing to show. Otherwise, since $a_i - 1 \geq 5$, the length of I_{i+1} is at most $\alpha_i |I_i|$, and $t^k(1/2)$ lies in I_{i+1} , we have that $\bar{t}_i(t^k(1/2)), \bar{t}_i^2(t^k(1/2)) \in I_i$ both lie to the right of $1/2$. Now we compute the Birkhoff sum at $\bar{t}_i^2(t^k(1/2))$. Let

$$l = k_i(t^k(1/2)) + k_i(\bar{t}_i(t^k(1/2)))$$

be the second return time of $t^k(1/2)$ to I_i . Then by (3) we have

$$S_{k+l}(1/2) = S_k(1/2) + \bar{f}_i(t^k(1/2)) + \bar{f}_i(\bar{t}_i(t^k(1/2))) = S_k(1/2) + 1 + (-1) = S_k(1/2) = m.$$

That is, the point $t^{k+l}(1/2) = \bar{t}_i^2(t^k(1/2)) \in I_i$ justifies the claim.

Now the theorem follows from this claim. By Proposition 2.1, the closure of the orbit of $(1/2, 0)$ contains $\{1/2\} \times \mathbb{Z}$. By the claim, for any $m \in \mathbb{Z}$, we may choose points $t^k(1/2)$ arbitrarily close to $1/2$ and *to the right* with $S_k(1/2) = m$. Consider any $\epsilon \in (0, 1/2)$ and a point $(x, m) \in S^1 \times \mathbb{Z}$. We want to show that for any $s \in \mathbb{Z}$, the orbit of $(1/2, s)$ contains a point in $[x, x + \epsilon) \times \{m\}$. Since α is irrational, the rotation t is minimal and there exists $k \geq 0$ with $t^k(1/2) \in [x, x + \frac{\epsilon}{2})$. Suppose that $S_k(1/2) = N$. The functions $\{f \circ t^i\}_{i=0}^k$ are individually constant on a short interval that has $1/2$ as its left endpoint, so there is $0 < \delta < \epsilon/2$ such that any point $y \in [1/2, 1/2 + \delta)$ satisfies $S_k(y) = S_k(1/2) = N$. By the claim, we can choose $l \geq 0$ such that

$$T^l(1/2, s) = (t^l(1/2), S_l(1/2)) \in \left[\frac{1}{2}, \frac{1}{2} + \delta\right) \times \{m - s - N\}.$$

Then

$$T^{l+k}(1/2, s) = (t^{l+k}(1/2), s + S_l(1/2) + S_k(t^l(1/2))).$$

As $t^l(1/2) \in [1/2, 1/2 + \delta)$ and $t^k(1/2) \in [x, x + \epsilon/2)$, we have

$$t^{l+k}(1/2) = t^k(t^l(1/2)) \in [t^k(1/2), t^k(1/2) + \delta) \subset [x, x + \epsilon).$$

In addition, $S_k(t^l(1/2)) = N$ by our choice of δ . It follows that $s + S_l(1/2) + S_k(t^l(1/2)) = s + (m - s - N) + N = m$ and $T^{l+k}(1/2, s) \in [x, x + \epsilon) \times \{m\}$, as desired. \square

Now we deduce Corollary 1.2 from Theorem 1.1.

Proof of Corollary 1.2. Theorem 1.1 is equivalent to the following major case of Corollary 1.2: For any $m \in \mathbb{Z}$, the partial orbit $\{t^n(1/2)\}_{n \in \Sigma(1/2, m)}$ is dense in S^1 . For the general case, for an arbitrary $k \in \mathbb{Z}$, we are interested in the density of the orbit points $t^{n+k}(1/2)$ with $n \in \Sigma(1/2, m)$, i.e. the image of the partial orbit $\{t^n(1/2)\}_{n \in \Sigma(1/2, m)}$ under the rotation t^k . Such a partial orbit is also dense in S^1 . \square

It remains to find the intervals I_i and prove Proposition 2.1. For this we proceed by induction. To construct I_{i+1} based on $J = I_i$ and its first return map, the inductive step fits into the following setup:

Assumption 2.2.

- We have chosen an interval $J \subset [0, 1)$ which contains $1/2$ and is centered at $1/2$.
- After scaling J by $1/|J|$ to unit length, the first return map to J , which we denote by t_J , is a rotation by a number $\beta = \pm[0; b, \dots]$ with $b \geq 5$ odd (so $|\beta| < 1/5$).

We construct a sub-interval J^{new} of J that is centered at $1/2$ with well-understood first return map among other properties. We describe the construction below in Lemmas 2.5 and 2.8, depending on the sign of β .

In the discussion below, we frequently look at different left-closed and right-open sub-intervals of $[0, 1)$ centered at $1/2$ and rescale them to length 1. To avoid confusion due to different scales, we use the following convention.

Convention 2.3. For a sub-interval J of $[0, 1)$ centered at $1/2$, we abuse notation and let $J : [0, 1) \rightarrow J$ be the unique affine homeomorphism fixing $1/2$. Then for any $x \in (0, 1)$, $J(x)$ is the point at distance x from the left endpoint of J after rescaling J to unit length. Similarly, $J[a, b)$ is the sub-interval of J corresponding to the interval $[a, b) \subset [0, 1)$ after rescaling J to unit length.

First case: $\beta > 0$

We first consider the case $\beta > 0$ and introduce some notation in order to state the inductive construction in Lemma 2.5. Note that the first coefficient $b = \lfloor 1/\beta \rfloor$. We partition J into sub-intervals

$$J_0 = J[0, \beta), J_1 = J[\beta, 2\beta), \dots, J_{b-1} = J[(b-1)\beta, b\beta), J_b = J[b\beta, 1),$$

each of which has length $\beta|J|$ except for J_b , which has length $\beta G(\beta)|J|$ where $G(x) = 1/x - \lfloor 1/x \rfloor$ as before. For a point $x \in J$, we have $t_J(x) = t^{k(x)}(x)$ where $k(x) = \inf\{k > 0 : t^k x \in J\}$, and by our induction hypothesis, $t_J(J(x)) = J(x + \beta \bmod 1)$ and $t_J(J_i) = J_{i+1}$ for all $0 \leq i < b-1$. We consider the orbit of $x \in J$ under t before its first return to J , and record the sequence of values of f along this orbit, namely

$$\mathcal{F}(x) = \{f(x), f(t(x)), \dots, f(t^{k(x)-1}(x))\}.$$

This is equivalent to recording the sequence of partial sums $\mathcal{S}(x) = \{S_i(x)\}_{i=1}^{k(x)}$ with $S_i(x) := \sum_{j=0}^{i-1} f(t^j(x))$. The partial sums keep track of the increment in the second coordinate (compared to (x, m)) along the orbit of (x, m) under T in the skew product:

$$\left\{ (x, m), T(x, m) = (tx, m + fx), \dots, T^{k(x)}(x, m) = (t^{k(x)}x, m + S_{k(x)}(x)) \right\}$$

Finally, we set $\Sigma(x) = S_{k(x)}(x)$, which is the total sum of the sequence $\mathcal{F}(x)$. We use $\mathcal{F}_1 \cdot \mathcal{F}_2$ to denote the concatenation of two sequences \mathcal{F}_1 and \mathcal{F}_2 .

Here are our remaining assumptions for the case $\beta > 0$ in addition to Assumption 2.2:

Assumption 2.4. There are sequences \mathcal{F}_+ , \mathcal{F}_- , and \mathcal{F}_0 with total sums 1, -1 , and 0, respectively, such that

- Whenever $x \in J[0, 1/2)$, we have $\mathcal{F}(x) = \mathcal{F}_+$,
- Whenever $x \in J[1/2, 1 - \beta)$, we have $\mathcal{F}(x) = \mathcal{F}_-$,
- Whenever $x \in J[1 - \beta, 1)$, we have $\mathcal{F}(x) = \mathcal{F}_- \cdot \mathcal{F}_0$.

Here we allow \mathcal{F}_0 to be an empty sequence.

As a consequence of the assumptions above, the sequence $\mathcal{S}(x)$ must be the sequence of partial sums for \mathcal{F}_+ , \mathcal{F}_- , or $\mathcal{F}_+ \cdot \mathcal{F}_0$ depending on the location of x as above. Denote the partial sum sequences of \mathcal{F}_+ and \mathcal{F}_- by \mathcal{S}_+ and \mathcal{S}_- , and denote the total sums of \mathcal{F}_+ , \mathcal{F}_- , \mathcal{F}_0 as Σ_+ , Σ_- , Σ_0 . The assumptions above imply $\Sigma_+ = 1$, $\Sigma_- = -1$, and $\Sigma_0 = 0$.

We record the maximum and minimum over each sequence of partial sums, i.e.

$$m_+ := \min \mathcal{S}_+, M_+ := \max \mathcal{S}_+, m_- := \min \mathcal{S}_-, M_- := \max \mathcal{S}_-$$

Our aim is to find a sub-interval $J^{\text{new}} \subset J$ containing and centered at $1/2$, for which the first return to J^{new} , rescaled by $1/|J^{\text{new}}|$, is a rotation by a new number $\beta^{\text{new}} = -[0; c, \dots]$ with $c \geq 3$ determined by β explicitly as in Lemma 2.5 below. Moreover, for $x \in J^{\text{new}}$, denote the first return time to J^{new} as

$$k^{\text{new}}(x) = \inf\{k > 0 : t^k(x) \in J^{\text{new}}\}$$

and consider as before the sequence of f -values

$$\mathcal{F}^{\text{new}}(x) := \{f(x), f(t(x)), \dots, f(t^{k^{\text{new}}(x)-1}(x))\}.$$

Let $\mathcal{S}^{\text{new}}(x)$ be the sequence of partial sums associated to $\mathcal{F}^{\text{new}}(x)$, and let $\Sigma^{\text{new}}(x) = S_{k^{\text{new}}(x)}(x)$ be the total sum.

The following lemma shows how we construct the sub-interval J^{new} and the nice properties guaranteed by the construction.

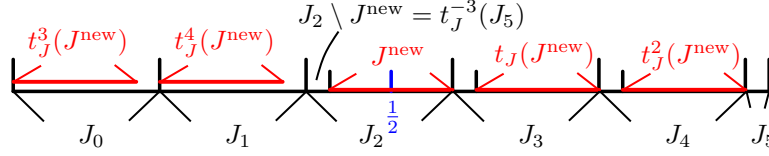


FIGURE 1. The decomposition of J into J_i 's when $b = 2n + 1 = 5$ for $n = 2$ and the orbit of J^{new} under iterations of t_J , for $\beta > 0$

Lemma 2.5. *Suppose there is a sub-interval $J \subset [0, 1)$ with first return map t_J satisfying Assumptions 2.2 and 2.4 with $\beta = [0; b, c + 1, \dots] > 0$, where $c \geq 3$. Denote $b = 2n + 1$ with $n \geq 1$. Then the sub-interval $J^{\text{new}} \subset J$ given by*

$$J^{\text{new}} := J \left[\frac{1}{2} - \frac{1}{2}\beta(1 - G(\beta)), \frac{1}{2} + \frac{1}{2}\beta(1 - G(\beta)) \right).$$

has the following properties:

- (1) J^{new} is symmetric about $1/2$ of length $\beta(1 - G(\beta))|J|$.
- (2) J^{new} is a sub-interval of J_n , the right endpoints of J^{new} and J_n are the same, and the left endpoint of J^{new} has distance $\beta G(\beta)|J| = |J_b|$ from the left endpoint of J_n .
- (3) The image of $J_n \setminus J^{\text{new}}$ under $n + 1$ iterations of t_J is J_b .
- (4) Re-scaling by $1/|J^{\text{new}}|$, the first return map to J^{new} is rotation by

$$\beta^{\text{new}} := -G(\beta)/(1 - G(\beta)) = -[0; c, \dots].$$

- (5) There are sequences

$$\mathcal{F}_+^{\text{new}} := \mathcal{F}_+ \cdot \mathcal{F}_-^n \cdot \mathcal{F}_0 \cdot \mathcal{F}_+^n, \quad \mathcal{F}_-^{\text{new}} := \mathcal{F}_-^{n+1} \cdot \mathcal{F}_0 \cdot \mathcal{F}_+^n, \quad \text{and} \quad \mathcal{F}_0^{\text{new}} := \mathcal{F}_+ \cdot \mathcal{F}_-^{n+1} \cdot \mathcal{F}_0 \cdot \mathcal{F}_+^n$$

satisfying:

- whenever $x \in J^{\text{new}}[0, \beta^{\text{new}})$ we have $\mathcal{F}^{\text{new}}(x) = \mathcal{F}_+^{\text{new}} \mathcal{F}_0^{\text{new}}$,
- whenever $x \in J^{\text{new}}[\beta^{\text{new}}, 1/2)$ we have $\mathcal{F}^{\text{new}}(x) = \mathcal{F}_+^{\text{new}}$,
- whenever $x \in J^{\text{new}}[1/2, 1)$ we have $\mathcal{F}^{\text{new}}(x) = \mathcal{F}_-^{\text{new}}$.

Moreover, $\mathcal{F}_+^{\text{new}}, \mathcal{F}_-^{\text{new}}, \mathcal{F}_0^{\text{new}}$ have total sums $1, -1, 0$ respectively.

Proof. Item (1) is immediate. To see item (2), note that $1/2$ lies in the interval $J_n = J[n\beta, (n+1)\beta)$ and its distances to the endpoints are

$$\left(\frac{1}{2} - n\beta \right) |J| = \frac{1}{2}(1 - 2n\beta)|J| = \frac{1}{2}\beta|J|(1 + G(\beta)) \quad \text{and} \quad \left((n+1)\beta - \frac{1}{2} \right) |J| = \frac{1}{2}\beta|J|(1 - G(\beta)).$$

Since t_J is rotation by $\beta|J| = |J_i|$ for $i < b$ and $t_J(J_i) = J_{i+1}$ for any $i < b - 1$, item (3) easily follows; see Figure 1.

Now we analyze the first return map. After scaling by $1/|J_n| = 1/\beta$, the first return map to J_n is rotation by $(b\beta - 1)/\beta = -G(\beta)$. Therefore, by restricting to the further sub-interval J^{new} and rescaling by $1/|J^{\text{new}}|$, one can check that the first return map to J^{new} is rotation by $\beta^{\text{new}} = -G(\beta)/(1 - G(\beta))$. This is essentially a simple case of Rauzy–Veech induction. See the next several paragraphs for more details. A direct computation verifies item (4), i.e.

$$\beta^{\text{new}} = -G(\beta)/(1 - G(\beta)) = -[0; c, \dots].$$

Next we compute the sequences $\mathcal{F}_+^{\text{new}}, \mathcal{F}_-^{\text{new}}, \mathcal{F}_0^{\text{new}}$. Note that by item (2) $t_J^k(J^{\text{new}})$ is a sub-interval of J_{n+k} sharing its right endpoint for $0 \leq k \leq n$ and $t_J^k(J^{\text{new}})$ is a sub-interval of $J_{k-(n+1)}$ sharing its left endpoint for $n+1 \leq k \leq 3n+1$; see Figure 1.

In particular, $t_J^{2n+1}(J^{\text{new}})$ lies in J_n sharing its left endpoint, and we observe that this completes the first return to J^{new} by t_J^{2n+1} for $x \in J^{\text{new}}[\beta^{\text{new}}, 1)$. Counting for which $0 \leq k \leq 2n$ we have $t_J^k(x)$ on the left or right of $J(1/2)$, we observe that, for $x \in J^{\text{new}}[\beta^{\text{new}}, 1/2)$, the sequence $\mathcal{F}^{\text{new}}(x)$ is equal to $\mathcal{F}_+^{\text{new}}$ defined as in (5), i.e.

$$\mathcal{F}_+^{\text{new}} = \mathcal{F}_+ \cdot \mathcal{F}_-^n \cdot \mathcal{F}_0 \cdot \mathcal{F}_+^n;$$

and for $x \in J^{\text{new}}[1/2, 1)$, the sequence $\mathcal{F}^{\text{new}}(x)$ is equal to $\mathcal{F}_-^{\text{new}}$ as in (5), i.e.

$$\mathcal{F}_-^{\text{new}} = \mathcal{F}_-^{n+1} \cdot \mathcal{F}_0 \cdot \mathcal{F}_+^n.$$

On the other hand, any $x \in J^{\text{new}}[0, \beta^{\text{new}})$ also returns to J_n for the first time via t_J^{2n+1} but lands in $J_n \setminus J^{\text{new}} = t_J^{2n+1}(J^{\text{new}}[0, \beta^{\text{new}}))$. After another $2n+2$ iterations of t_J , x finally returns to J^{new} and the additional sequence of f -values is $\mathcal{F}_0^{\text{new}}$ as in (5), i.e.

$$\mathcal{F}_0^{\text{new}} = \mathcal{F}_+ \cdot \mathcal{F}_-^{n+1} \cdot \mathcal{F}_0 \cdot \mathcal{F}_+^n.$$

Indeed, after the first return to J_n (i.e. $2n+1$ iterations of t_J), x lands to the right of $1/2$ for the next $n+1$ iterations of t_J in J rather than n times as before, since $t_J^{n+1}(J_n \setminus J^{\text{new}}) = J_b$. Finally, the last $n+1$ iterations take such x back to J^{new} and x stays on the left of $1/2$ until it is back.

Therefore, for $x \in J^{\text{new}}[0, \beta^{\text{new}})$, we see that $\mathcal{F}^{\text{new}}(x)$ is the concatenation $\mathcal{F}_+^{\text{new}} \cdot \mathcal{F}_0^{\text{new}}$ as claimed in item (5). The computations above in these three cases together verify item (5), where the total sums of the sequences $\mathcal{F}_+^{\text{new}}, \mathcal{F}_-^{\text{new}}, \mathcal{F}_0^{\text{new}}$ are $1, -1, 0$, respectively, as an immediate corollary of the expressions in (5) and the total sums of $\mathcal{F}_+, \mathcal{F}_-, \mathcal{F}_0$ given in Assumption 2.4. \square

Now consider the partial sum sequences $\mathcal{S}_+^{\text{new}}$ and $\mathcal{S}_-^{\text{new}}$ for the sequences $\mathcal{F}_+^{\text{new}}$ and $\mathcal{F}_-^{\text{new}}$, respectively. We estimate the upper and lower bounds of these partial sum sequences:

$$M_+^{\text{new}} := \max \mathcal{S}_+^{\text{new}}, m_+^{\text{new}} := \min \mathcal{S}_+^{\text{new}}, M_-^{\text{new}} := \max \mathcal{S}_-^{\text{new}}, m_-^{\text{new}} := \min \mathcal{S}_-^{\text{new}}.$$

Lemma 2.6. *For the sequences $\mathcal{F}_+^{\text{new}}, \mathcal{F}_-^{\text{new}}$ and the integer n defined as in Lemma 2.5, assuming the total sums of $\mathcal{F}_+, \mathcal{F}_-,$ and \mathcal{F}_0 to be $1, -1, 0$ respectively as in Assumption 2.4, and assuming $n \geq 2$ (i.e. $b \geq 5$), we have*

- $M_+^{\text{new}} \geq M_+$;
- $m_+^{\text{new}} \leq m_- - (n-2)$;
- $M_-^{\text{new}} \geq M_-$;
- $m_-^{\text{new}} \leq m_- - n$;

Proof. These easily follow by inspection and the fact that $\Sigma_+ = +1, \Sigma_- = -1$. As $\mathcal{F}_+^{\text{new}}$ starts with the sequence \mathcal{F}_+ , we note that \mathcal{S}_+ is a prefix of the sequence $\mathcal{S}_+^{\text{new}}$, which verifies the first bullet. The third bullet follows similarly.

For the second bullet, consider the expression

$$\mathcal{F}_+^{\text{new}} = (\mathcal{F}_+ \cdot \mathcal{F}_-^{n-1}) \cdot \mathcal{F}_- \cdot (\mathcal{F}_0 \cdot \mathcal{F}_+^n).$$

The sequence $\mathcal{F}_+ \cdot \mathcal{F}_-^{n-1}$ has total sum $\Sigma_+ + (n-1)\Sigma_- = -(n-2)$, so for the subsequence \mathcal{F}_- after these terms, its partial sum sequence \mathcal{S}_- shifted by $-(n-2)$ appears as a subsequence of $\mathcal{S}_-^{\text{new}}$, which implies the second bullet.

The last bullet can be shown analogously, as the sequence $\mathcal{F}_-^{\text{new}}$ starts with $(\mathcal{F}_-)^n \cdot \mathcal{F}_-$, where the part in parentheses has total sum $n\Sigma_- = -n$. \square

Second case: $\beta < 0$

We now consider the case $\beta < 0$. Denote $\gamma = -\beta$. Then the first return map to J is $t_J(J(x)) = J(x - \gamma \bmod 1)$. The case here is essentially just mirroring the case above, as now we are rotating to the left. For clarity, we include some details below. Define the sequences $\mathcal{F}(x)$ and $\mathcal{S}(x)$ as before for any $x \in J$ and let $\Sigma(x)$ be the total sum of $\mathcal{F}(x)$. Here are the remaining assumptions for the case $\beta < 0$.

Assumption 2.7. There are sequences $\mathcal{F}_+, \mathcal{F}_-, \mathcal{F}_0$ with total sums $\Sigma_+ = 1, \Sigma_- = -1, \Sigma_0 = 0$, respectively, such that

- For $x \in J[0, \gamma)$ we have $\mathcal{F}(x) = \mathcal{F}_+ \cdot \mathcal{F}_0$.
- For $x \in J[\gamma, 1/2)$ we have $\mathcal{F}(x) = \mathcal{F}_+$.

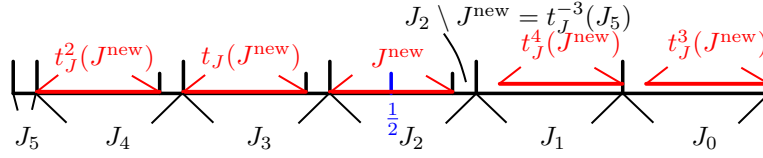


FIGURE 2. The decomposition of J into J_i 's when $b = 2n + 1 = 5$ for $n = 2$ and the orbit of J^{new} under iterations of t_J , for $\beta < 0$.

- For $x \in J[1/2, 1)$ we have $\mathcal{F}(x) = \mathcal{F}_-$.

We denote the first coefficient by $b = \lfloor 1/\gamma \rfloor$, and express it as $b = 2n + 1$ for some $n \geq 2$. We again partition J into intervals

$$J_0 = J[1 - \gamma, 1), J_1 = J[1 - 2\gamma, 1 - \gamma), \dots, J_b = J[0, 1 - b\gamma),$$

and we have $t_J(J_i) = J_{i+1}$ for $0 \leq i < b - 1$. The interval J_b has length $\gamma G(\gamma)$.

Our aim is again to find a sub-interval $J^{new} \subset J$ containing $1/2$ and symmetric about $1/2$, for which the first return to J^{new} inherits nice properties regarding the sequence $\mathcal{F}^{new}(x)$ of f -values and the sequence $\mathcal{S}^{new}(x)$ of partial sums, defined just as in the previous case.

Lemma 2.8. *Suppose there is a sub-interval $J \subset [0, 1)$ with first return map t_J satisfying Assumptions 2.2 and 2.7 with $\beta = -\gamma = -[0; b, c + 1, \dots] < 0$, where $c \geq 3$. Denote $b = 2n + 1$ with $n \geq 1$. Then with notation as above, the sub-interval $J^{new} \subset J$ given by*

$$J^{new} := J \left[\frac{1}{2} - \frac{1}{2}\gamma(1 - G(\gamma)), \frac{1}{2} + \frac{1}{2}\gamma(1 - G(\gamma)) \right).$$

has the following properties:

- (1) J^{new} is symmetric about $1/2$ of length $\gamma(1 - G(\gamma))|J|$.
- (2) J^{new} is a sub-interval of J_n , the left endpoints of J^{new} and J_n are the same, and the right endpoint of J^{new} has distance $\gamma G(\gamma)|J| = |J_b|$ from the right endpoint of J_n .
- (3) The image of $J_n \setminus J^{new}$ under $n + 1$ iterations of t_J is J_b .
- (4) Re-scaling by $1/|J^{new}|$, the first return map to J^{new} is rotation by

$$\beta^{new} := G(\gamma)/(1 - G(\gamma)) = [0; c, \dots].$$

- (5) There are sequences

$$\mathcal{F}_+^{new} := \mathcal{F}_+^{n+1} \cdot \mathcal{F}_0 \cdot \mathcal{F}_-^n, \quad \mathcal{F}_-^{new} := \mathcal{F}_- \cdot \mathcal{F}_+^n \cdot \mathcal{F}_0 \cdot \mathcal{F}_-^n, \quad \text{and} \quad \mathcal{F}_0^{new} := \mathcal{F}_- \cdot \mathcal{F}_+^{n+1} \cdot \mathcal{F}_0 \cdot \mathcal{F}_-^n$$

with total sums $1, -1, 0$, respectively, satisfying:

- whenever $x \in J^{new}[0, 1/2)$ we have $\mathcal{F}^{new}(x) = \mathcal{F}_+^{new}$,
- whenever $x \in J^{new}[1/2, 1 - \beta^{new})$ we have $\mathcal{F}^{new}(x) = \mathcal{F}_-^{new}$,
- whenever $x \in J^{new}[1 - \beta^{new}, 1)$ we have $\mathcal{F}^{new}(x) = \mathcal{F}_-^{new} \mathcal{F}_0^{new}$.

Proof. The proof is almost the same as that of Lemma 2.5, by symmetry; see Figure 2. So we just summarize a few key points below. Items (1)–(3) are just direct computations as before, noting that $1/2$ lies in the interval J_n but $|J_b|$ -closer to its left endpoint this time.

As in the previous case, after scaling by $1/|J_n| = 1/\gamma$, the first return map to J_n is rotation by $(1 - b\gamma)/\gamma = G(\gamma)$, which is now positive. Thus, by restricting further to the sub-interval J^{new} and rescaling by $1/|J^{new}|$ instead, the first return to J^{new} is rotation by $\beta^{new} = G(\gamma)/(1 - G(\gamma))$ as in item (4).

Item (5) follows by an analysis of first returns to J^{new} , which is just mirroring the case of $\beta > 0$: the interval $t_J^{2n+1}(J^{new})$ lies in J_n sharing the right endpoint, completing the first return to J^{new} for all $x \in J^{new}[0, 1 - \beta^{new})$, and the sequence of f -values depends on whether x lies on the left or right of $1/2$, which only changes the first term (\mathcal{F}_\pm) in the concatenation. For those $x \in J^{new}[1 - \beta^{new}, 1)$, it takes another $2n + 2$ iterations of t_J to return to J^{new} , resulting in the additional sequence \mathcal{F}_0^{new} . \square

As before, for the partial sum sequences \mathcal{S}_+ and \mathcal{S}_- denote

$$M_+ := \max \mathcal{S}_+, \quad m_+ := \min \mathcal{S}_+, \quad M_- := \max \mathcal{S}_-, \quad m_- := \min \mathcal{S}_-,$$

and similarly for the partial sum sequences $\mathcal{S}_+^{\text{new}}$ and $\mathcal{S}_-^{\text{new}}$ by adding superscripts everywhere in the above equations.

The proof of the following lemma is similar to that of Lemma 2.6, using the expressions for $\mathcal{F}_+^{\text{new}}$ and $\mathcal{F}_-^{\text{new}}$ in Lemma 2.8.

Lemma 2.9. *For the sequences $\mathcal{F}_+^{\text{new}}$, $\mathcal{F}_-^{\text{new}}$, and the integer n defined as in Lemma 2.8, assuming the total sums of \mathcal{F}_+ , \mathcal{F}_- , and \mathcal{F}_0 to be 1, -1 , 0 , respectively, as in Assumption 2.7, and assuming $n \geq 2$, we have*

- $M_+^{\text{new}} \geq M_+ + n$;
- $m_+^{\text{new}} \leq m_+$;
- $M_-^{\text{new}} \geq M_- + (n - 2)$;
- $m_-^{\text{new}} \leq m_-$.

Finally we can prove Proposition 2.1.

Proof of Proposition 2.1. We inductively construct I_i and check the first three items as follows. For the base case $i = 1$, set $I_1 = [0, 1)$ and $\beta_1 = \alpha$. Then the three items are either obvious or vacuous. Since the first coefficient of α is odd, Assumptions 2.2 and 2.4 hold for the rotation $t_J = t$ on $J = I_1$, where $\mathcal{F}_+ = \{1\}$, $\mathcal{F}_- = \{-1\}$, and $\mathcal{F}_0 = \emptyset$ is the empty sequence. By Lemma 2.5, we have a sub-interval $I_2 := J^{\text{new}}$ symmetric about $1/2$ of length less than $\alpha_1|I_1|$, for which the first return map is rotation by $\beta^{\text{new}} = -\alpha_2$, where α_2 is defined in formula (2.1).

Note that the first return map on I_2 with the sequences $\mathcal{F}_+^{\text{new}}$, $\mathcal{F}_-^{\text{new}}$, and $\mathcal{F}_0^{\text{new}}$ from Lemma 2.5 satisfies Assumptions 2.2 and 2.7. Thus Lemma 2.8 produces a sub-interval I_3 symmetric about $1/2$ of length less than $\alpha_2|I_2|$, for which the first return map is rotation by α_3 , with new sequences of f -values satisfying Assumptions 2.2 and 2.4.

We continue this process to define I_i inductively, alternating between applications of Lemma 2.5 and Lemma 2.8 to I_i with i odd and even, respectively. Namely, given I_i and α_i , define $I_{i+1} = I_i^{\text{new}}$ and $\alpha_{i+1} = \alpha_i^{\text{new}}$. Item (5) in Lemmas 2.5 and 2.8 ensures item (3) in Proposition 2.1.

Define inductively \mathcal{F}_+^i , \mathcal{F}_-^i , \mathcal{F}_0^i as the sequences of f -values for first returns to I_i , using $\mathcal{F}_\pm^{i+1} = (\mathcal{F}_\pm^i)^{\text{new}}$ and similarly for \mathcal{F}_0^{i+1} . Let \mathcal{S}_\pm^i be the sequences of partial sums of \mathcal{F}_\pm^i . Let M_\pm^i and m_\pm^i be the bounds on the partial sums \mathcal{S}_\pm^i estimated in Lemmas 2.6 and 2.9.

Finally we prove (4). We first prove below that there are points $t^k(1/2) \in I_1$ in the forward orbit of $1/2$ with $S_k(1/2)$ equal to any given integer m . We will explain at the end how to find such points in I_j for any $j \in \mathbb{Z}_+$ instead of I_1 . Note that the sequence \mathcal{S}_-^i consists exactly of the Birkhoff sums of $1/2$ that occur before $1/2$ returns to I_i for the first time. We have $M_-^i = \max \mathcal{S}_-^i$ and $m_-^i = \min \mathcal{S}_-^i$. Thus, it suffices to prove that $M_-^i \rightarrow +\infty$ and $m_-^i \rightarrow -\infty$ as $i \rightarrow \infty$.

Since the first coefficient $a_i - 1$ (or a_1 when $i = 1$) of α_i is odd and at least 5 by assumption, $n_i := (a_i - 2)/2 \geq 2$ (and $n_1 := (a_1 - 1)/2 \geq 2$). We have $m_-^{2i} \leq m_-^{2i-1} - n_{2i-1} \leq m_-^{2i-1} - 2$ by Lemma 2.6 and $m_-^{2i+1} \leq m_-^{2i}$ by Lemma 2.9. It follows that $m_-^{i+2} \leq m_-^i - 2$ for all i and hence $\lim m_-^i = -\infty$. For a similar reason, $\lim M_+^i = +\infty$, which we now use to deduce that $\lim M_-^i = +\infty$. In fact, we have $M_-^{2i+2} \geq M_-^{2i+1} \geq M_+^{2i} + (n_{2i} - 2) \geq M_+^{2i}$ by Lemmas 2.6 and 2.9. Thus $\lim M_-^i = +\infty$ and $\lim m_-^i = -\infty$ as claimed.

The proof above works in the same way after replacing α by α_j , I_1 by I_j , f by \bar{f}_j , and t by \bar{t}_j for any $j \in \mathbb{Z}_+$. That is, there is $k \in \mathbb{Z}_+$ such that $\bar{t}_j^k(1/2) \in I_j$ with \bar{t}_j -Birkhoff sum equal to m . As \bar{t}_j is the first return map to I_j , such a point in I_j is also in the forward orbit of $1/2$ under t , and its \bar{t}_j -Birkhoff sum is equal to the corresponding t -Birkhoff sum, which completes the proof. \square

The same method can be used to study the Birkhoff sum along other orbits. We give a sketch for one explicit example below, which we use later to find a leaf that is not dense in Theorem 1.3.

Example 2.10. Fix $m \geq 2$. Let $\alpha = [0; 2m+1, 2m+2, 2m+2, \dots]$ (i.e. $a_1 = 2m+1$ and $a_n = 2m+2$ for all $n \geq 2$), which satisfies the assumption of Theorem 1.1. We consider the orbit of $x = (1+\alpha)/2$ and claim that $S_n(x) \leq 0$ for all $n \in \mathbb{Z}$. Here we set $S_0(x) = 0$ and $S_{-n}(x) = -\sum_{k=1}^n f(t^{-k}(x))$ for any $n > 0$ so that $T^n(x, s) = (t^n(x), s + S_n(x))$ for all $n \in \mathbb{Z}$. The claim implies that the (forward and backward) orbit of $(x, 0)$ under iterations of T always has non-positive second coordinate.

We sketch a proof of the claim. First, note that we can take care of the backward orbit by symmetry. In fact, for our particular x we have $t^{-(n+1)}(x) = 1 - t^n(x)$ for all $n > 0$, i.e. the backward orbit (starting at $t^{-1}(x) = (1-\alpha)/2$) and the forward orbit (starting at x) are symmetric around $1/2$, and thus the sequences of f -values along the forward and backward orbits differ by a negative sign. It follows that $S_{-n}(x) = S_n(x)$ for all $n \in \mathbb{Z}_+$. So it suffices to check that $\max_{n \geq 1} S_n(x) \leq 0$.

To compute $S_n(x)$ with $n > 0$, we use the same renormalization procedure with the nested intervals $I_1 \supset I_2 \supset \dots$ as above. Let \mathcal{F}_\pm^i and \mathcal{F}_0^i (resp. \mathcal{S}_\pm^i and \mathcal{S}_0^i) be the sequence of f -values (resp. partial sums) defined inductively as in the proof above. Let $M_\pm^i = \max \mathcal{S}_\pm^i$ and $M_0^i = \max \mathcal{S}_0^i$. A direct computation shows that $t^m(x) = 1 - \frac{1}{2}\alpha G(\alpha)$ and $t^{2m+1}(x) = (m+1)\alpha - \frac{1}{2}\alpha G(\alpha)$, so the forward orbit enters I_2 for the first time after $2m+1$ iterations of t . In I_2 -coordinates, we have $t^{2m+1}(x) = I_2(y)$ with

$$y = \frac{[(m+1)\alpha - \frac{1}{2}\alpha G(\alpha)] - [m\alpha + \alpha G(\alpha)]}{\alpha(1 - G(\alpha))} = \frac{\alpha - \frac{3}{2}\alpha G(\alpha)}{\alpha(1 - G(\alpha))} = 1 - \frac{1}{2}\beta,$$

where $\beta = G(\alpha)/(1 - G(\alpha))$ and the first return map $\bar{t}_2 : I_2 \rightarrow I_2$ is rotation by $-\beta$ in I_2 -coordinates by Lemma 2.5. Our choice of α makes $\beta = \alpha$. Then applying the first return map \bar{t}_2 another m times we arrive at $I_2(1 - (m+1/2)\beta)$, at which point we land in I_3 for the first time. In I_3 -coordinates, this is $I_3(z)$ with

$$z = \frac{[1 - (m+1/2)\beta] - [1 - (m+1)\beta]}{\beta(1 - G(\beta))} = \frac{1}{2}(1 + \gamma),$$

where $\gamma = G(\beta)/(1 - G(\beta))$. Noting that $\gamma = \beta = \alpha$ by our choice of α , we see $z = x$, so are now exactly at $I_3(x)$, and the first return map to I_3 is rotation by $\gamma = \alpha$ in I_3 -coordinates by Lemma 2.8. Thus from here on the analysis repeats. It follows that the sequence of f -values along the forward orbit is given by

$$(2.2) \quad [(\mathcal{F}_-^1)^{m+1} \cdot (\mathcal{F}_+^1)^m \cdot (\mathcal{F}_-^2)^m] \cdot [(\mathcal{F}_-^3)^{m+1} \cdot (\mathcal{F}_+^3)^m \cdot (\mathcal{F}_-^4)^m] \dots$$

The Birkhoff sums are the partial sums of this sequence, and to analyze them we compute M_\pm^k and M_0^k for all $k \geq 1$. The idea of the computation is similar to the proof of Lemmas 2.6 and 2.9, which yields the following recursive formulas for our particular α :

$$M_+^{2k} = M_+^{2k-1}, \quad M_-^{2k} = M_-^{2k-1}, \quad M_0^{2k} = M_+^{2k-1},$$

and

$$M_+^{2k+1} = M_0^{2k} + m + 1, \quad M_-^{2k+1} = M_0^{2k} + m - 1, \quad M_0^{2k+1} = M_0^{2k} + m,$$

for all $k \geq 1$. Then by induction, we have

$$M_+^{2k-1} = (m+1)k - m, \quad M_-^{2k-1} = (m+1)k - m - 2, \quad M_0^{2k-1} = (m+1)k - m - 1,$$

for all $k \geq 2$ and

$$M_+^{2k} = (m+1)k - m, \quad M_-^{2k} = (m+1)k - m - 2, \quad M_0^{2k} = (m+1)k - m,$$

for all $k \geq 1$. Now by examining the sequence in formula (2.2) bracket by bracket, it is straightforward to check that $\max_{n \geq 1} S_n(x) = -1$.

3. BACKGROUND ON LAMINATIONS AND RAYS

We recall some background on geodesic laminations and geodesic rays on hyperbolic surfaces. Let X be a complete oriented hyperbolic surface without boundary. We will typically consider the case that X is of the *first kind*. This means that the limit set of $\pi_1(X)$ acting on the universal cover $\widehat{X} \cong \mathbb{H}^2$ is the entire Gromov boundary $\partial X \cong S^1$. A *geodesic lamination* Λ on X is a closed subset of X consisting of pairwise disjoint, simple, complete geodesics. Each such complete geodesic is called a *leaf* of Λ .

In Section 4, we will construct laminations on hyperbolic surfaces using train tracks, weight systems, and foliated rectangles. Here is the necessary background. A *train track* τ on X is a locally finite graph embedded on X with the following additional structure. At any vertex v of τ , the set $\mathcal{B}(v)$ of edges incident to v has a circular order induced from the orientation of X . We have a partition of $\mathcal{B}(v)$ into a pair of non-empty sets $\mathcal{B}_i(v)$ and $\mathcal{B}_o(v)$ which we call incoming and outgoing, respectively, such that the total order defined by any $g \in \mathcal{B}_o(v)$ (resp. $g \in \mathcal{B}_i(v)$) restricts to the same order on $\mathcal{B}_i(v)$ (resp. $\mathcal{B}_o(v)$) independent of g . For $e, f \in \mathcal{B}_i(v)$, we write $e < f$ if and only if (e, f, g) is counterclockwise at v for any $g \in \mathcal{B}_o(v)$. For $e, f \in \mathcal{B}_o(v)$, we write $e < f$ if and only if (e, f, g) is clockwise at v for any $g \in \mathcal{B}_i(v)$. The edges of τ are called *branches* and the vertices of τ are called *switches*. A *train path* t on τ is a finite or infinite path immersed in τ with the property that at every switch v , t enters v through $\mathcal{B}_i(v)$ and exits v through $\mathcal{B}_o(v)$, or vice versa.

A *weight system* on τ is a function $w : \mathcal{B}(\tau) \rightarrow \mathbb{R}_+$ satisfying the switch equations: for any switch v of τ we have

$$\sum_{e \in \mathcal{B}_i(v)} w(e) = \sum_{f \in \mathcal{B}_o(v)} w(f).$$

Associated to the pair (τ, w) we construct the following *union of foliated rectangles*. For each $b \in \mathcal{B}(\tau)$ we assign a rectangle $R(b) = [0, w(b)] \times [0, 1]$. We glue the rectangles at each switch v as follows. For any switch v of τ we consider the interval $I(v) = [0, \ell]$ where

$$\ell = \sum_{b \in \mathcal{B}_i(v)} w(b) = \sum_{b \in \mathcal{B}_o(v)} w(b).$$

Suppose that $b_1 < \dots < b_n$ are the outgoing branches at v . Then $I(v)$ is divided into consecutive closed intervals I_1, \dots, I_n of lengths $w(b_1), \dots, w(b_n)$, respectively, where $0 \in I_1$ and the I_i 's overlap only on their boundaries. Then we glue $[0, w(b_i)] \times \{0\} \subset R(b_i)$ via an orientation-preserving isometry to the interval I_i . Similarly, $I(v)$ is also divided into intervals J_1, \dots, J_m of lengths $w(c_1), \dots, w(c_m)$ where c_1, \dots, c_m are the incoming branches at v . Then we glue $[0, w(c_j)] \times \{1\} \subset R(c_j)$ to J_j via an orientation-preserving isometry. The union of foliated rectangles \mathcal{F} for (τ, w) is the quotient of the disjoint union of the rectangles $R(b)$ and intervals $I(v)$ by these gluing relations.

Each rectangle $R(b)$ of \mathcal{F} is foliated by the vertical segments $\{v\} \times [0, 1]$ for $v \in [0, w(b)]$. This endows \mathcal{F} with the structure of a singular foliation. The singularities are the points where at least three rectangles of \mathcal{F} meet. In fact, at most four rectangles can meet, in which case we have two rectangles on both sides of an interval $I(v)$. By thickening $I(v)$ to a rectangle, we assume exactly three rectangles meet at each singularity. A *leaf* ℓ of \mathcal{F} is an embedding of \mathbb{R} into \mathcal{F} that is the union of a sequence

$$\dots \sigma_{-1} \sigma_0 \sigma_1 \dots$$

of vertical line segments $\sigma_i = \{v_i\} \times [0, 1] \subset R(b_i)$ with consecutive segments meeting at endpoints, and which satisfies the following conditions. First, we require that $\dots b_{-1} b_0 b_1 \dots$ is a train path of τ . Second, we have an additional requirement when the leaf contains at least two singularities, which we now describe. Given an orientation of a leaf ℓ , singularities on ℓ fall into two types, merging or splitting; see Figure 3. Moreover, singularities along ℓ must alternate between the two types as they arise from gluing of rectangles. At a merging singularity, there are two possible local pictures of ℓ ,

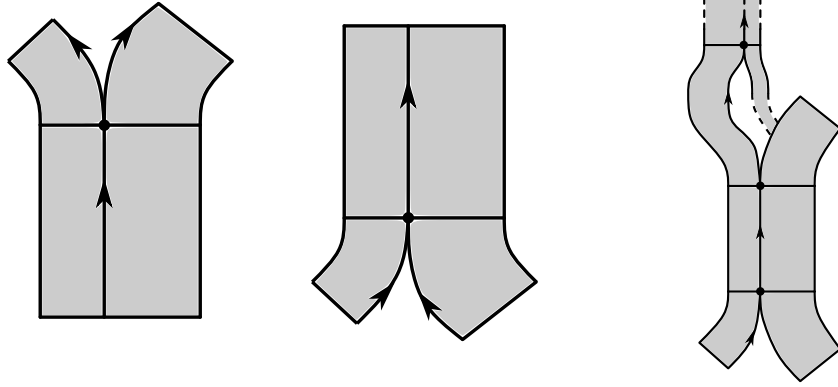


FIGURE 3. Left: two singular leaves that split after passing through a splitting singularity; middle: two singular leaves that merge after passing through a merging singularity; right: a singular leaf (indicated by the arrows) passes through three singularities and always splits to the left and merges from the left.

namely merging from the left or right branch. Similarly, at a splitting singularity, ℓ splits to the left or right branch. For a leaf ℓ containing at least two singularities, we require a choice of *left* or *right*: either ℓ always merges from the left and splits to the left, or it always merges from the right and splits to the right; see Figure 3. A leaf will be called *singular* if it contains a singularity and *non-singular* otherwise. We will use unions of foliated rectangles in Section 4 to construct geodesic laminations on hyperbolic surfaces.

Finally, suppose that X has an isolated puncture p . A ray ℓ is any complete simple geodesic asymptotic to p on at least one end. The ray ℓ is a *loop* if it is asymptotic to p on both ends. A ray is *filling* if it intersects every loop based at p . Denote by $\mathcal{R}(X; p)$ the graph whose vertices are the rays based at p , and whose edges join pairs of rays that are disjoint. By [5], the graph $\mathcal{R}(X; p)$ consists of uncountably many connected components. Among these components, exactly one is of infinite diameter and Gromov hyperbolic. The remaining components are *cliques* of rays. These cliques consist of pairwise disjoint rays, each of which intersects every ray not lying in the clique. A ray in such a clique connected component is called *high-filling*. The set of cliques of high-filling rays is identified with the Gromov boundary $\partial\mathcal{R}(X; p)$ [5, Theorem 6.3.1]. If a ray is filling but not high-filling then it is called *2-filling* [5, Lemma 5.6.4]. Thus there is a trichotomy: a ray is either not filling, 2-filling, or high-filling. As such, 2-filling rays can be thought of as *fake boundary points* for the graph $\mathcal{R}(X; p)$, with properties mimicking those of high-filling rays. Finally, note that a priori the graph $\mathcal{R}(X; p)$ depends on the particular hyperbolic metric X . However, if Y is a different first kind complete hyperbolic surface homeomorphic to X , then there is a natural bijection between the rays on X based at p and the rays on Y based at p ; see the end of Part 1 in [5]. This bijection preserves the property of a ray being a loop, 2-filling, high-filling, etc. Hence we may actually define $\mathcal{R}(S; p) := \mathcal{R}(X; p)$ where S is the underlying topological surface to X , and the graph $\mathcal{R}(S; p)$ is well-defined independent of a particular first kind hyperbolic metric on S . When S is the plane minus a Cantor set then 2-filling rays exist, and the construction can be applied to many other surfaces of infinite type [7]. Theorem 1.4 now confirms their existence on any infinite type surface with at least one isolated puncture.

4. LAMINATIONS

We consider the train track τ illustrated in Figure 4. The weights of three branches are labeled for some $\alpha \in (0, 1)$. The weights of the other branches are determined by these via the switch

equations. Associated to these weights on τ , we construct the standard *union of foliated rectangles* F . There is a single branch of weight 1 in τ which gives rise to a rectangle R of F .

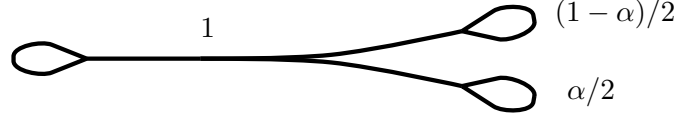


FIGURE 4. A weighted train track τ . The second return map to a horizontal interval in the rectangle R of the union of foliated rectangles F is a rotation by α .

The train track τ has an infinite cyclic cover $\tilde{\tau}$ which is pictured in Figure 5. The weights on τ pull back to weights on $\tilde{\tau}$, some of which are labeled in Figure 5.

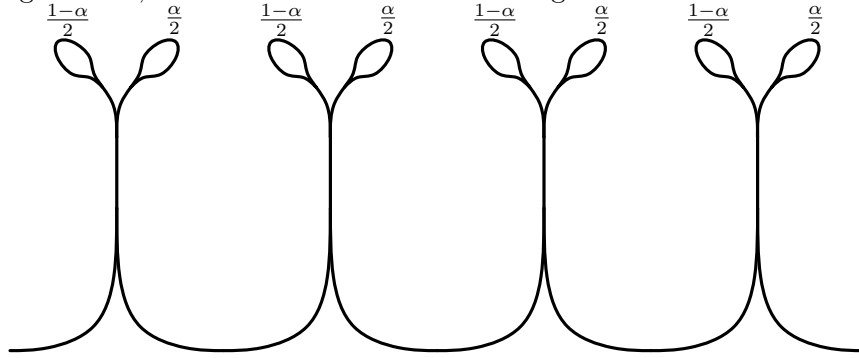


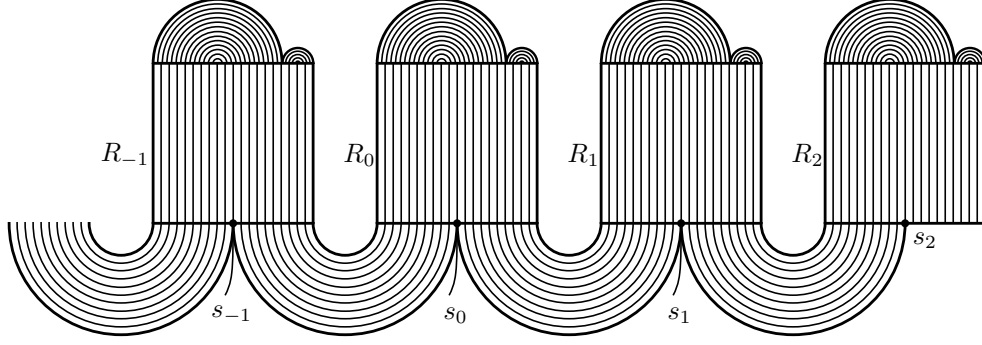
FIGURE 5. The infinite cyclic cover $\tilde{\tau}$ of τ .

We consider the union of foliated rectangles \tilde{F} for $\tilde{\tau}$ with the described weights; see Figure 6. Then \tilde{F} is an infinite cyclic cover of F . The branches of $\tilde{\tau}$ of weight 1 give rise to a sequence of rectangles $\dots, R_{-1}, R_0, R_1, \dots$ in \tilde{F} which are indexed by \mathbb{Z} and cover the rectangle R of F corresponding to the branch of τ with weight 1. We choose the numbering so that there is a rectangle joining R_i to R_{i+1} and a rectangle joining R_i to R_{i-1} for each i , both with width $1/2$. For the rectangle of width $1/2$ joining R_i and R_{i+1} , one of its boundary leaves (the lower boundary in Figure 6) extends to a singular leaf ℓ_i in \tilde{F} passing through the singularities s_i and s_{i+1} . The leaves ℓ_{i-1} and ℓ_i share a ray r_i starting at s_i . The following consequence of Corollary 1.2 is crucial to our construction of an infinite clique of 2-filling rays.

Lemma 4.1. *Suppose that $\alpha \in (0, 1)$ satisfies the conditions of Theorem 1.1. Then for each i , the ray r_i of \tilde{F} is dense in \tilde{F} , hence so is the singular leaf ℓ_i .*

Proof. To prove this, we parameterize the disjoint union $\bigcup_{i \in \mathbb{Z}} R_i$ by $[0, 1]^2 \times \mathbb{Z}$, where R_i is isometrically identified with the unit square $[0, 1]^2$ and the leaves of \tilde{F} intersect the rectangles $[0, 1]^2$ in vertical segments $\{x\} \times [0, 1]$. We further choose the orientation on the vertical segments such that the singularity s_i is given by $(1/2, 0, i)$ in these coordinates and each r_i starts from s_i by going upwards; see Figure 6.

After r_i passes through R_i for the first time, it travels downwards in R_i along the vertical segment with coordinate $(1 - \alpha) - 1/2 = 1/2 - \alpha$ since $\alpha < 1/2$ as in Theorem 1.1. Thus r_i passes through $(1/2 - \alpha, 0, i)$ to exit R_i . At this point, r_i will enter R_{i-1} since $1/2 - \alpha < 1/2$, and it travels upwards starting at $(1 - 1/2 + \alpha, 0, i - 1) = (1/2 + \alpha, 0, i - 1)$.

FIGURE 6. Part of the union of foliated rectangles \tilde{F}

In general, if at some point the ray r_i is traveling upwards in some R_j along the vertical segment with coordinate $x \in (0, 1)$, it hits the top of R_j and then starts to travel downwards in R_j along $\{b(x)\} \times [0, 1]$, where

$$b(x) = \begin{cases} 1 - \alpha - x & \text{if } x < 1 - \alpha, \\ 2 - \alpha - x & \text{if } x > 1 - \alpha. \end{cases}$$

Note that $b(x) = 1 - t(x)$, where $t = t_\alpha$ is the rotation by α as in the introduction, that is, $t(x) \in (0, 1)$ is the fractional part of $x + \alpha$. At this point, r_i exits R_j at $(b(x), 0, j)$ and enters $R_{j'}$ with $j' = j + 1$ if $b(x) > 1/2$ and $j' = j - 1$ if $b(x) < 1/2$. That is, $j' = j + f(t(x))$ for the function $f = \chi_{[0, 1/2)} - \chi_{[1/2, 1]}$ as in the definition of the transformation T in Theorem 1.1. Moreover, r_i enters $R_{j'}$ by traveling upwards along the vertical segment with coordinate $1 - b(x) = t(x)$.

In the calculations above, we ignored all boundary cases since we only care about $x = t^n(1/2)$ for some $n \geq 0$ and α is irrational.

It follows from the analysis above that r_i visits the n -th rectangle with entry point

$$(t^{n-1}(1/2), 0, i + \sum_{j=1}^{n-1} f(t^j(1/2))).$$

The sum $\sum_{j=1}^{n-1} f(t^j(1/2))$ is equal to $S_n(1/2) - f(1/2) = S_n(1/2) + 1$ where S_n is the n -th Birkhoff sum defined in the introduction. Thus, r_i contains the points $(t^{n-1}(1/2), 0, i + 1 + S_n(1/2))$ for $n \geq 1$, and the pairs $(t^{n-1}(1/2), i + 1 + S_n(1/2))$ are dense in $[0, 1] \times \mathbb{Z}$ by Corollary 1.2. To see the last claim, note that for each $m \in \mathbb{Z}$, the set of $n \geq 0$ with $i + 1 + S_n(1/2) = m$ is $\Sigma(1/2, m - i - 1)$, so the pairs above contain $(t^n(1/2), m)$ for all $n \in \Sigma(1/2, m - i - 1) - 1$ except possibly $n = 0$, and the first coordinates of such pairs are dense by Corollary 1.2. This proves that r_i is dense in R_m for any $m \in \mathbb{Z}$ and hence dense in the whole foliation \tilde{F} . This completes the proof of Lemma 4.1. \square

We now define a geodesic lamination on an infinite type hyperbolic surface. The track $\tilde{\tau}$ may be folded to yield the train track $\hat{\tau}$ pictured on the left of Figure 7. The track $\hat{\tau}$ is carried by another track σ shown on the right of Figure 7, which can in turn be embedded in any infinite type surface Σ with at least one isolated puncture p as we explain below; see the left of Figure 8.

On the left of Figure 8, every tiny black disk represents a subsurface of Σ with a single boundary component, corresponding to the boundary of the black disk. We require each such subsurface to have either positive genus or at least two punctures. Furthermore, in Σ the border line pictured on the left of Figure 8 is glued to itself by a reflection across the central vertical line, so that Σ has no boundary. With this identification, each dotted horizontal line segment represents an essential simple closed curve γ_i on Σ . Thus, the surface Σ with the black disks removed is a flute surface Σ' . Any infinite-type surface without boundary and with at least one isolated puncture can be realized

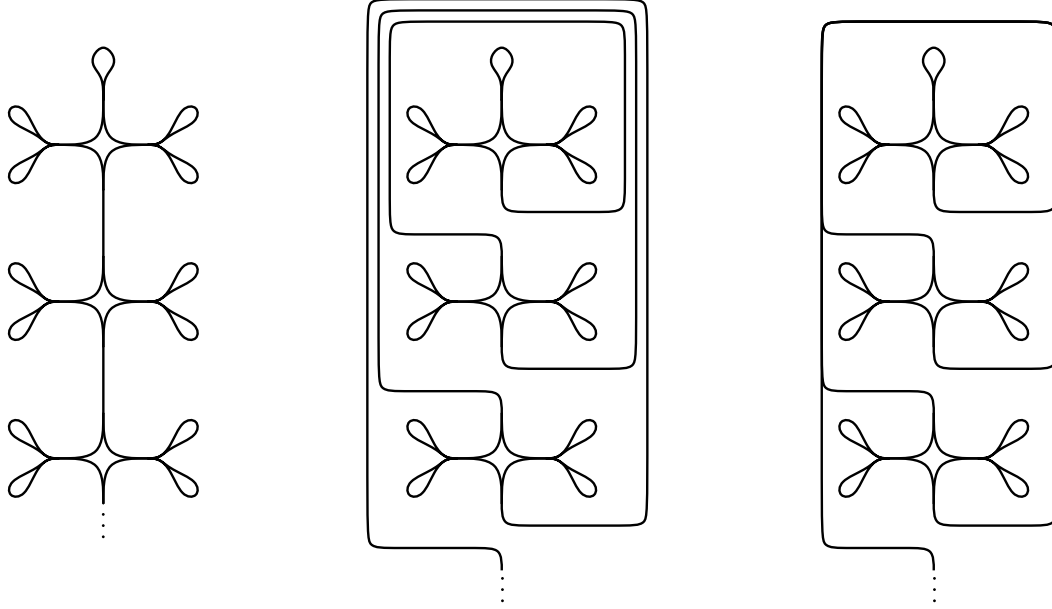


FIGURE 7. Left: The track $\hat{\tau}$ obtained by folding $\tilde{\tau}$; Middle: Another embedding of $\tilde{\tau}$ that spirals; Right: The track σ obtained by collapsing parallel branches.

this way by appropriately choosing the topological type of the subsurfaces represented by the black disks.

Lemma 4.2. *For any orientable surface S of infinite type with at least one isolated puncture p , there is a sequence of surfaces $\{D_i\}_{i \geq 1}$ each with one boundary component and either positive genus or at least two punctures, so that the surface (Σ, p) above with the black disks homeomorphic to the D_i 's is homeomorphic to (S, p) .*

Proof. Recall the classification of (possibly non-compact) orientable surfaces without boundary [9]. Each surface S has a space of ends E , which is totally disconnected, compact, and metrizable. The non-planar ends form a closed subset $E_g \subset E$, which is nonempty if and only if S has infinite genus. Then the classification states that two surfaces are homeomorphic if and only if they have the same genus (possibly infinite) and the pairs of spaces of ends (E, E_g) are homeomorphic. Moreover, given any pair (E, E_g) with E totally disconnected, compact, and metrizable and $E_g \subset E$ closed, and given $n \in \mathbb{Z}_{\geq 0} \cup \{\infty\}$ so that $n < \infty$ iff $E_g = \emptyset$, there is an orientable surface S with genus n and spaces of ends homeomorphic to (E, E_g) . We say S is of infinite type if either E is an infinite set or E_g is nonempty.

Consider any S of infinite type with an isolated puncture p , and denote its space of ends by E . Since p is isolated, $E \setminus \{p\}$ is clopen. There are two cases:

- (1) Suppose E is infinite. Then there is an accumulation point $x \in E$ and a sequence of nested clopen neighborhoods $E \setminus \{p\} = V_1 \supset V_2 \supset \dots$ of x with $\bigcap_i V_i = \{x\}$. Up to relabelling, we may assume that $U_i := V_i \setminus V_{i+1}$ contains at least two points for all $i \geq 1$. For each $i \geq 1$, there is a surface S_i with space of ends homeomorphic to $(U_i, U_i \cap E_g)$. Moreover, if $U_i \cap E_g = \emptyset$, then we can choose S_i to have any genus $n_i \in \mathbb{Z}_{\geq 0}$, which we now specify. If S has finite genus, we may choose the n_i 's so that $\sum n_i$ is equal to the genus of S . If S has infinite genus, for each i with $U_i \cap E_g = \emptyset$, we choose $n_i = 0$ if x is planar and $n_i > 0$ if x is non-planar. Let D_i be S_i with an open disk removed. Then each D_i either has positive genus or has at least two punctures. Choose the black disks in the construction of our surface Σ above to be homeomorphic to the surfaces D_i . Then (Σ, p) is homeomorphic to (S, p) by the classification of surfaces.

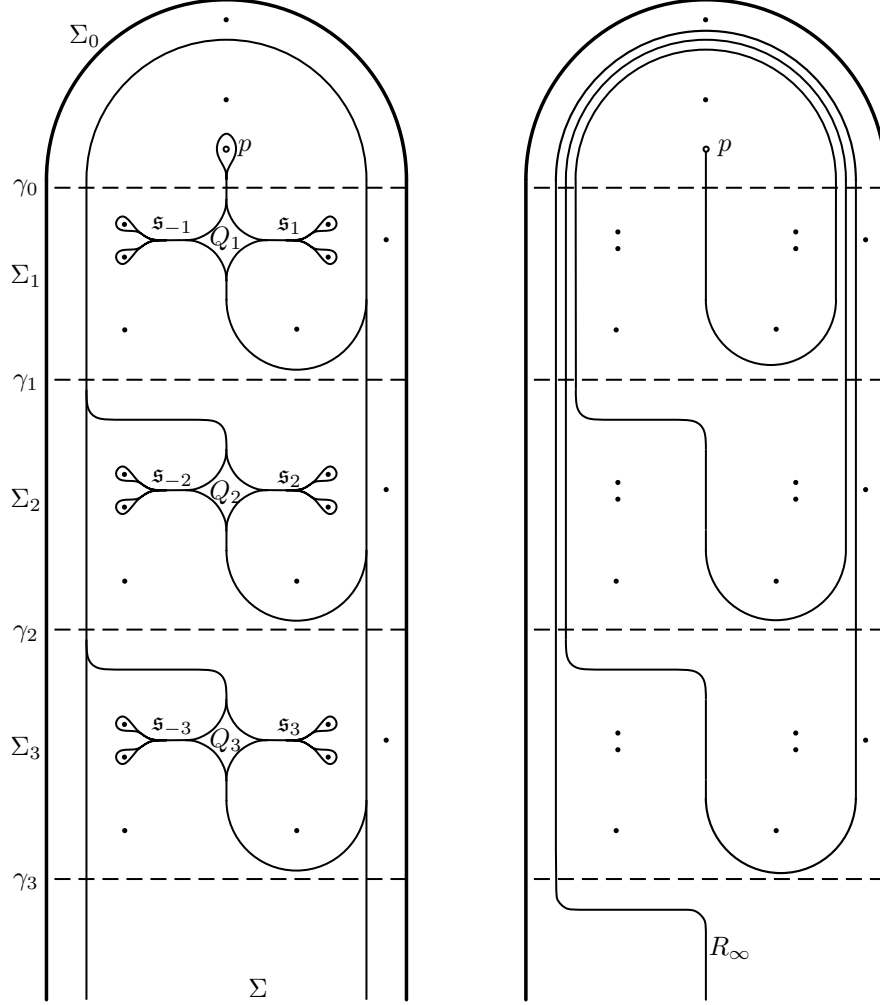


FIGURE 8. Left: The track σ obtained by embedding $\hat{\tau}$ on an infinite type surface Σ and collapsing parallel branches. Right: The non-filling ray R_∞ on Σ .

- (2) Suppose E is finite. Then E_g must be nonempty for S to be of infinite type. Then $E = E_g \sqcup E' \sqcup \{p\}$ where E' consists of planar ends other than p . For $1 \leq i \leq |E_g| - 1$, let S_i be the surface of infinite genus and exactly one (non-planar) end, i.e. the Loch Ness monster. For $i = |E_g|$, let S_i be the surface of genus one with $|E'|$ punctures. For $i > |E_g|$, let S_i be the torus. Now for each $i \in \mathbb{Z}_+$, let D_i be S_i with an open disk removed. Choose the black disks in the construction of our surface Σ above to be homeomorphic to the surfaces D_i . Then Σ has infinite genus and has the same pair of spaces of ends as S , so again (Σ, p) is homeomorphic to (S, p) by the classification of surfaces.

□

The simple closed curves $\{\gamma_i\}_{i \geq 0}$ cut Σ' into an infinite sequence of finite type subsurfaces $\{\Sigma_i\}_{i \geq 0}$. For each $i \geq 1$ (resp. $i = 0$), the surface Σ_i is bounded by two (resp. one) γ_i 's together with 7 (resp. 2) boundary components of black disks (resp. and a puncture p). Thus each Σ_i admits a complete hyperbolic structure with geodesic boundary components all of length 1. In the sequel, we choose the metric on Σ_i with the additional property that the (finitely many) train paths in $\sigma \cap \Sigma_i$ have lengths bounded above independent of i , which can be done for instance by making Σ_i ($i \geq 1$) all isometric under the obvious translation in Figure 8. Since each black disk represents a surface

with positive genus or at least two punctures, it admits a hyperbolic structure of the first kind so that the boundary is a geodesic of length 1. Hence by gluing, we can endow Σ with a complete hyperbolic metric of the first kind so that

- (1) each γ_i is a closed geodesic of length 1,
- (2) the train paths in $\sigma \cap \Sigma_i$ have lengths bounded above independent of i .

Let $\tilde{\Sigma} \cong \mathbb{H}^2$ be the universal cover of Σ . Consider the preimage $\tilde{\sigma}$ of σ and the collection \mathcal{L} of lifts of all γ_i 's to $\tilde{\Sigma}$. We notice the following fact:

Lemma 4.3. *For the choice of hyperbolic metric on Σ above, there are uniform constants $K, C > 0$ such that any bi-infinite train path of $\tilde{\sigma}$ is a (K, C) -quasi-geodesic. In particular, it limits to two distinct points on the Gromov boundary $\partial\tilde{\Sigma}$.*

Proof. We show this by looking at the intersections with lines in \mathcal{L} . Each lift of γ_i is a bi-infinite geodesic in \mathcal{L} . Note that there is a lower bound on the distance between any two lines of \mathcal{L} by the collar lemma since the γ_i 's have bounded length. Moreover, the segment between any two consecutive intersections of the train path with \mathcal{L} is a lift of a train path in $\sigma \cap \Sigma_i$ for some i , and thus its length is bounded above by a uniform constant due to our choice of metric.

We claim that any train path of $\tilde{\sigma}$ with endpoints on two lines of \mathcal{L} is not homotopic, relative to endpoints, into a line in \mathcal{L} . Given the claim, any bi-infinite train path of $\tilde{\sigma}$ intersects a bi-infinite non-backtracking sequence of geodesics in \mathcal{L} at a uniformly bounded linear rate, from which the lemma follows.

The claim above follows from the observations below. There are only two homeomorphism classes of pairs $(\Sigma_i, \Sigma_i \cap \sigma)$. Moreover, in each track $\Sigma_i \cap \sigma$, there are finitely many train paths. Finally, by the choice of γ_i 's, no train path of $\Sigma_i \cap \sigma$ is homotopic into $\partial\Sigma_i$ via a homotopy keeping the endpoints of the train path on the boundary, and no two distinct train paths of $\Sigma_i \cap \sigma$ are homotopic via such a homotopy. \square

Consequently any bi-infinite train path t of $\tilde{\sigma}$ may be straightened to a geodesic α in $\partial\tilde{\Sigma}$ with the same endpoints on the Gromov boundary. Moreover, the proof above implies that the sequences of lines in \mathcal{L} intersecting α and t , respectively, are identical. In addition, the intersections with \mathcal{L} cut both α and t into segments of length bounded above and below by uniform constants. We also see from the last observation made in the proof above that if t_1, t_2 are train paths in $\tilde{\sigma}$ such that t_i joins a line $L_i \in \mathcal{L}$ to a line $L'_i \in \mathcal{L}$, then t_1 and t_2 are equal if and only if $L_1 = L_2$ and $L'_1 = L'_2$. The following lemmas can be deduced from these facts.

Lemma 4.4. *Let $\{t_i\}_{i=1}^\infty$ be bi-infinite train paths of $\tilde{\sigma}$ straightening to geodesics $\{\alpha_i\}_{i=1}^\infty$ of $\tilde{\Sigma}$. If α is a geodesic of $\tilde{\Sigma}$ such that $\alpha_i \rightarrow \alpha$, then α intersects infinitely many lines in \mathcal{L} at each end.*

Proof. Suppose this is not the case. Then one end of α projects to a geodesic ray in Σ disjoint from the curves γ_j . Note that each α_i projected to Σ is disjoint from the boundary curve of each black disk in Figure 8. Hence the limiting ray above is also disjoint from such boundary components. So the ray must be trapped in some Σ_j . This implies that there is an arbitrarily long geodesic segment β_i inside Σ_j in the projection of α_i for i sufficiently large. This contradicts the observation we made above, that α_i is divided by \mathcal{L} into segments of uniformly bounded length. \square

Lemma 4.5. *Let $\{t_i\}_{i=1}^\infty$ be bi-infinite train paths of $\tilde{\sigma}$ straightening to geodesics $\{\alpha_i\}_{i=1}^\infty$ of $\tilde{\Sigma}$. Suppose that α is a geodesic of $\tilde{\Sigma}$. Then $\alpha_i \rightarrow \alpha$ if and only if α is also carried by $\tilde{\sigma}$ and for any finite sub-path s of the train path t defining α , s is contained in t_i for all large enough i . In particular, the set of geodesics carried by $\tilde{\sigma}$ is closed in the space of geodesics of $\tilde{\Sigma}$.*

Proof. We only focus on the less obvious direction: If α_i converges to a geodesic α , then α is carried by $\tilde{\sigma}$ and for any finite sub-path s of the train path t defining α , s is contained in t_i for all large enough i .

Each α_i intersects a bi-infinite sequence of lines in \mathcal{L} . By Lemma 4.4 and the fact that intersection is an open condition, these sequences (with an appropriate choice of the 0-th term) are pointwise eventually constant, with the limiting sequence equal to the lines in \mathcal{L} intersecting α . As each straightening α_i intersects the same sequence of lines in \mathcal{L} as the corresponding train path t_i does, the limiting sequence above determines a train path t carrying α with the desired properties. \square

Lemma 4.6. *Let s and t be bi-infinite train paths of $\tilde{\sigma}$ straightening to geodesics β and α . Then β and α share an endpoint $q \in \partial\tilde{\Sigma}$ if and only if s and t share an infinite train path limiting to q .*

Proof. We again focus on the less obvious direction: If β and α share an endpoint $q \in \partial\tilde{\Sigma}$, then s and t share an infinite train path limiting to q . As in the proof above, α intersects the same bi-infinite sequence of lines in \mathcal{L} as t does. Note that the endpoints of these lines must converge to q since lines in \mathcal{L} are at distances uniformly bounded away from zero. This implies that this sequence of lines would eventually all intersect the ray in β limiting to q , and vice versa. It easily follows that s and t intersect the same sequence of lines in \mathcal{L} at one end, determining the desired infinite train path. \square

Now we define a geodesic lamination on Σ as follows. Recall that the weights on τ induce weights on $\tilde{\tau}$. Via the union of foliated rectangles construction, the leaves of the rectangles glue to a set of train paths on $\tilde{\tau}$ and they correspond to a set $\tilde{\mathcal{T}}$ of train paths on σ via the carrying map. Finally, we consider the train path t_* in σ which passes through each surface Σ_i ($i > 0$) exactly twice and never returns. This is the train path parallel to the border line on the left side of Figure 8. We define $\mathcal{S} := \tilde{\mathcal{T}} \cup \{t_*\}$, a set of train paths on σ . By Lemma 4.3, we may straighten the train paths in \mathcal{S} to geodesics. Denote the resulting set of geodesics by Λ . Since the train paths in \mathcal{S} do not cross, neither do the geodesics of Λ .

Lemma 4.7. *The set of geodesics Λ is closed as a subset of Σ . Therefore it is a geodesic lamination on Σ .*

We postpone the proof of Lemma 4.7 and first discuss the train paths in \mathcal{S} in more detail. Any nonsingular leaf of \tilde{F} uniquely determines a train path in σ , and it is determined by any segment of the leaf contained in a foliated rectangle of \tilde{F} . Now we describe train paths of $\tilde{\mathcal{T}}$ corresponding to singular leaves of \tilde{F} . Note that there is a sequence of quadrilaterals Q_i in the complement of the train track σ ; see the left of Figure 8. In each Q_i , $i \geq 1$, a pair of singularities \mathfrak{s}_i and \mathfrak{s}_{-i} sit at the two opposite horizontal corners, corresponding to the singularities s_i and s_{-i+1} in Figure 6. For each $i \in \mathbb{Z}_+$, there is a unique singular leaf ℓ_i containing \mathfrak{s}_i and \mathfrak{s}_{i+1} and a unique singular leaf ℓ_{-i} containing \mathfrak{s}_{-i} and \mathfrak{s}_{-i-1} . Moreover, there is a singular leaf ℓ_0 containing \mathfrak{s}_{-1} and \mathfrak{s}_1 . Thus, we have a collection $\dots, \ell_{-1}, \ell_0, \ell_1, \dots$ of singular leaves of \tilde{F} indexed by the integers, corresponding to the ones investigated in Lemma 4.1. This gives rise to a collection $\dots, t_{-1}, t_0, t_1, \dots$ of train paths in \mathcal{S} . Note that for each $i \in \mathbb{Z}$, ℓ_i shares a ray with ℓ_{i-1} and ℓ_{i+1} , respectively, so that t_i shares a half-infinite sub-train-path with t_{i-1} and t_{i+1} , respectively.

For each i , the train path t_i gives rise to a leaf L_i of Λ , corresponding to the leaf ℓ_i in \tilde{F} studied in Lemma 4.1.

Proof of Lemma 4.7. Lift Λ to a set of geodesics $\tilde{\Lambda}$ on $\tilde{\Sigma}$. Let $\lambda_1, \lambda_2, \dots$ be geodesics in $\tilde{\Lambda}$ converging to the geodesic λ . By Lemma 4.5, λ is carried by $\tilde{\sigma}$. Let t be a train path of $\tilde{\sigma}$ straightening to λ . If t projects to t_* in Σ then λ is in $\tilde{\Lambda}$ by definition. Otherwise, t passes through some branch b on the boundary of a quadrilateral in the complement of $\tilde{\sigma}$. Hence, t_i passes through b for i sufficiently large. Without loss of generality we assume that t_i passes through b for every i .

Lift \tilde{F} to a foliation of a subset of $\tilde{\Sigma}$. Then for each i , t_i is the train path defined by a (possibly singular) leaf of \tilde{F} . That is, after collapsing the rectangles of \tilde{F} to branches, and composing with the carrying map to $\tilde{\sigma}$, we obtain t_i . Thus, for each t_i there is a unique vertical line segment

u_i in the rectangle $R(b)$ which the leaf corresponding to t_i passes through. Up to passing to a subsequence, the segments u_i converge to a vertical segment u in $R(b)$, and we may further assume all segments u_i lie on the same side of u , say the left side (for a chosen orientation of u). Let r_i be the (possibly singular) leaf defining t_i (which passes through u_i). Furthermore, let r be the (possibly singular) leaf which passes through u , and, when given the orientation induced by u , merges from or splits into the left rectangle at every singularity that it passes through (if there are indeed any such singularities). Then u_i converges to u , since for any finite sequence of rectangles that u passes through, u_i also passes through the same sequence for i sufficiently large. Hence t_i converges to the train path defined by u , which is therefore equal to t . In particular, λ is a leaf of $\tilde{\Lambda}$. \square

The following lemma is the key to obtain our infinite clique of 2-filling rays.

Lemma 4.8. *The complementary component to Λ containing p is a once-punctured ideal polygon with countably infinitely many ends, exactly one of which is the limit of the others. The sides of the ideal polygon are the leaves $\{L_i\}_{i \in \mathbb{Z}}$.*

In order to prove Lemma 4.8, we look at some particular rays, which we denote as R_i with $i \in \mathbb{Z} \cup \{\infty\}$. We apologize for reusing the notation and warn the reader not to confuse them with the rectangles R_i discussed earlier (which play no role in the rest of the paper).

First we define a ray R_∞ with one end at the isolated puncture p . This is the geodesic ray pictured on the right of Figure 8. It is non-proper and not filling (as defined at the end of Section 3). Observe that it is disjoint from Λ .

We also define a sequence of geodesic rays R_i for $i \in \mathbb{Z} \setminus \{0\}$ as follows. The ray R_i is obtained by following R_∞ until it enters the quadrilateral Q_i with ends corresponding to the singularities $\mathfrak{s}_{\pm i}$. Thereafter, it passes through \mathfrak{s}_i and follows the common half-infinite sub-train-path of t_{i-1} and t_i (if $i > 0$) or of t_i and t_{i+1} (if $i < 0$). The path just described may be homotoped to be simple and disjoint from any given leaf of Λ , and furthermore, none of its arcs in a component of $\Sigma \setminus \sqcup_i \gamma_i$ is homotopic into the boundary. Hence the path may be straightened to a geodesic ray R_i ; see Figure 9.

Now we prove Lemma 4.8.

Proof. Recall that the surfaces Σ_j are the complementary subsurfaces of the dotted curves γ_j and black disks in Figure 8. We see that for $i \gg 0$ or $i \ll 0$, R_i and R_∞ pass through many of the surfaces Σ_j in the same order, and in each such Σ_j , the arcs of R_i and R_∞ are homotopic, keeping endpoints on the boundary. Hence we have $R_i \rightarrow R_\infty$ as $i \rightarrow \infty$ and as $i \rightarrow -\infty$. Furthermore, R_i is asymptotic to L_i and L_{i-1} if $i > 0$ and R_i is asymptotic to L_i and L_{i+1} if $i < 0$. Finally, the rays R_i occur in the order

$$R_\infty < \dots < R_2 < R_1 < R_{-1} < R_{-2} < \dots < R_\infty$$

in the circular order on geodesics asymptotic to p .

Lift R_∞ to a ray \tilde{R}_∞ in the universal cover $\tilde{\Sigma}$. Then \tilde{R}_∞ has one endpoint at a lift \tilde{p} of p on $\partial\tilde{\Sigma}$ and the other endpoint at a point $z \in \partial\tilde{\Sigma}$. Let g be a generator of the cyclic subgroup of $\pi_1(\Sigma)$ fixing \tilde{p} . There is a unique lift \tilde{R}_i of R_i based at \tilde{p} , between \tilde{R}_∞ and $g \cdot \tilde{R}_\infty$. Up to replacing g by g^{-1} , we see that $\tilde{R}_i \rightarrow g\tilde{R}_\infty$ as $i \rightarrow +\infty$ and $\tilde{R}_i \rightarrow \tilde{R}_\infty$ as $i \rightarrow -\infty$. Moreover, there is a lift \tilde{L}_i , for $i \in \mathbb{Z}$, such that

- $\tilde{L}_0, \tilde{R}_{-1}, \tilde{R}_1$ are the sides of an ideal triangle;
- $\tilde{L}_i, \tilde{R}_i, \tilde{R}_{i+1}$ are the sides of an ideal triangle for $i > 0$;
- $\tilde{L}_i, \tilde{R}_i, \tilde{R}_{i-1}$ are the sides of an ideal triangle for $i < 0$.

Consequently, \tilde{R}_∞ , $g\tilde{R}_\infty$, and the \tilde{L}_i 's form the sides of a polygon with countably infinitely many ends. Each of these ends is isolated except z and gz , which are limits of the others. After quotienting

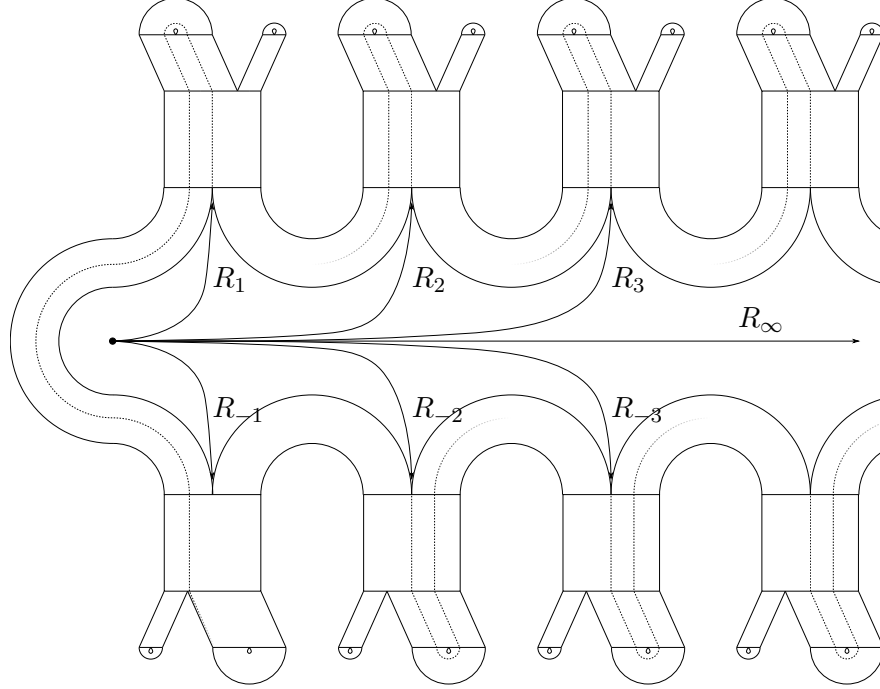


FIGURE 9. The rays R_i and R_∞ . They enter the union of foliated rectangles at a cusp and thereafter follow a leaf of the corresponding singular foliation (the dotted lines in the figure). For ease of presentation, the picture has been “unwrapped” before being embedded into Σ .

by g , we obtain a once-punctured ideal polygon with a countable set of ends, exactly one of which is the limit of the others, as claimed. \square

Finally we prove Theorems 1.3 and 1.4.

Proof of Theorem 1.4. By Lemma 4.2, any infinite type surface S with at least one isolated puncture p is homeomorphic to our surface Σ by a suitable choice in the construction. Construct the lamination Λ and use the notation as above. We see from Lemma 4.8 that every simple ray based at p , except R_i for $i \in \{\infty\} \cup \mathbb{Z} \setminus \{0\}$, intersects L_i for some $i \in \mathbb{Z}$. Moreover, L_i has a half leaf asymptotic to R_i , and this half leaf is dense in Λ by Lemma 4.1. Hence each R_i accumulates onto Λ . Thus, every simple ray based at p , not contained in $\{R_i\}_{i \in \{\infty\} \cup \mathbb{Z} \setminus \{0\}}$ intersects R_i for every $i \in \mathbb{Z} \setminus \{0\}$. Thus each ray R_i is 2-filling, only disjoint from one non-filling long ray R_∞ , and $\{R_i\}_{i \in \mathbb{Z} \setminus \{0\}}$ is an infinite clique of 2-filling rays. \square

Proof of Theorem 1.3. Let $S = \Sigma$ with the hyperbolic structure and lamination Λ as above. In the construction of Λ , choose $\alpha = [0; 2m+1, 2m+2, 2m+2, \dots]$ as in Example 2.10 for some $m \geq 2$, which satisfies the assumptions of Theorem 1.1. Each leaf L_i described above is dense in Λ by Lemma 4.1, so Λ is topologically transitive. On the other hand, the full orbit we examined in Example 2.10 has (forward and backward) Birkhoff sum always non-positive, so the corresponding leaf misses infinitely many rectangles, and thus it is not dense. There is an obvious \mathbb{Z} action on \tilde{F} in Figure 6. It is straightforward to see that the \mathbb{Z} -orbit of this leaf yields infinitely many distinct non-dense leaves, which completes our proof. \square

REFERENCES

- [1] Javier Aramayona, Ariadna Fossas, and Hugo Parlier. Arc and curve graphs for infinite-type surfaces. *Proc. Amer. Math. Soc.*, 145(11):4995–5006, 2017.

- [2] Juliette Bavard. Hyperbolicité du graphe des rayons et quasi-morphismes sur un gros groupe modulaire. *Geom. Topol.*, 20(1):491–535, 2016.
- [3] Juliette Bavard. An infinite clique of high-filling rays in the plane minus a cantor set, 2021.
- [4] Juliette Bavard and Alden Walker. The Gromov boundary of the ray graph. *Trans. Amer. Math. Soc.*, 370(11):7647–7678, 2018.
- [5] Juliette Bavard and Alden Walker. Two simultaneous actions of big mapping class groups. *Trans. Amer. Math. Soc.*, 376(11):7603–7650, 2023.
- [6] Michael Boshernitzan and David Ralston. Continued fractions and heavy sequences. *Proc. Amer. Math. Soc.*, 137(10):3177–3185, 2009.
- [7] Lvzhou Chen and Alexander J. Rasmussen. Laminations and 2-filling rays on infinite type surfaces. *Ann. Inst. Fourier (Grenoble)*, 73(6):2305–2369, 2023.
- [8] David Ralston. $1/2$ -heavy sequences driven by rotation. *Monatsh. Math.*, 175(4):595–612, 2014.
- [9] Ian Richards. On the classification of noncompact surfaces. *Trans. Amer. Math. Soc.*, 106:259–269, 1963.

DEPARTMENT OF MATHEMATICS, PURDUE UNIVERSITY, WEST LAFAYETTE, IN, USA
Email address, L. Chen: `lvzhou@purdue.edu`

DEPARTMENT OF MATHEMATICS, STANFORD UNIVERSITY, STANFORD, CA, USA
Email address, A.J. Rasmussen: `ajrasmus@stanford.edu`